

Ultrafast Laser Material Damage Simulation—A New Look at an Old Problem

AARTI OJHA

Research Scholar, Physics, Sangam Universty , Bhilwara

DR. ABHISHEK SAXENA

Assistant Professor, Physics, Sangam Universty , Bhilwara

DR. KAMAL CHAND JAIN

Professor, Physics, M.L.V.T.E.C, Bhilwara

ABSTRACT

The objective of the current research is to examine the effects of a laser beam on a specimen made from composite material. The materials investigated are CFRP, GFRP, PMMA, and structural steel. The CAD model of a specimen is produced in Creo design software & transient thermal analysis is undertaken to utilize ANSYS FEA software.

The kerf width and HAZ are obtained for all the specimens i.e., CFRP, GFRP, PMMA, and structural steel. The HAZ is highest for steel material and is minimum for PMMA and GFRP. The HAZ for PMMA and GFRP is limited to kerf width. For CFRP material, the maximum temperature obtained at 1 mm distance from laser beam incident is 5412.7K and maximum temperature at 2mm distance from laser beam incident is 3408.1K

Laser cutting is used in manufacturing industries and is used for various materials .The incident laser beam increases the temperature and also affects the nearby regions. This heat-affected region is different for ductile materials and other composite materials. It is essential to investigate the heataffected zone which incurs a change in elastic-plastic behavior. The objective of the current research is to examine the effects of a laser beam on a specimen made from composite material. The materials investigated are CFRP, GFRP, PMMA, and structural steel. The CAD model of a specimen is produced in Creo design software & transient thermal analysis is undertaken to utilize ANSYS FEA software.

Keywords: Laser cutting, FEA, Thermal Analysis

Lasers: Fundamentals, Types, and Operations

The acronym LASER, constructed from *Light Amplification by Stimulated Emission of Radiation*, has become so common and popular in every day life that it is now referred to as *laser*. Fundamental theories of lasers, their historical development from milliwatts to petawatts in terms of power, operation principles, beam characteristics, and applications of laser have been the subject of several books [1 – 5]. Introduction of lasers, types of laser systems and their operating principles, methods of generating extreme ultraviolet/vacuum ultraviolet (EUV/VUV) laser lights, properties of laser radiation, and modification in basic structure of lasers are the main sections of this chapter.

Modification in Basic Laser Structure

Addition of some electronic, optical, or electro-optical systems between the active media and mirror to modify the pulse width, pulse shape, and energy/pulse and generation of integral multiple of laser frequency is important for advanced technological applications. Mode locking or phase locking, Q-switching, pulse shaping, pulse compression and expansion, frequency multiplication, and so on, are some commonly used methods in advanced laser technology.

Basic Principle of Mode Locking

Mode locking is a technique in optics by which a laser can be made to produce light pulses of extremely short duration of the order of picoseconds (10^{-12} s) or femtosec-onds (10^{-15} s). The basis of this technique is to induce constant phase relationship between the modes of laser cavity. Simply, same phase of δ can be chosen for all laser modes. Such a laser is called *mode-locked* or *phase-locked laser*, which produces a train of extremely narrow laser pulses separated by equal time intervals. Let N modes are oscillating simultaneously in the laser cavity with $(A_0)_n$, ω_n , and δ_n being the ampli-tude, angular frequency, and phase of the n th mode. All these parameters vary with time, therefore modes are incoherent. The output of such laser is a linear combi-

N

nation of n different modes and is given by $A(t) = \sum_{n=0}^{N-1} (A_0)_n e^{i(\omega_n t + \delta_n)}$ expression.

For simplicity, frequency of the n th mode can be written as $\omega_n = \omega - n$, where ω_n is the mode with highest frequency and $= c\pi/L$ is the angular frequency separation between two modes. If all the modes have same amplitude and we force the various modes to maintain same relative phase δ to one another, that where $\varphi = \pi ct/L$.

that δ is, we mode lock the laser such N is, then the expression for resultant amplitude will be $A(t) = A_0 e^{i(\omega t + \delta)}$ $\sum_{n=0}^{N-1} e^{-i\pi nct/L} = A_0 e^{i(\omega t + \delta)} \sin(N\varphi/2)/\sin(\varphi/2)$,

The irradiance of the laser output is given by $I(t) = A(t)A(t)^* =$

$A_0^2 \sin^2(N\phi/2)/\sin^2(\phi/2)$, which is the periodic function of the period $= 2\pi$ in the time interval $t = 2L/c$ (time of round-trip inside the cavity). The maximum value of

irradiance is $N^2 A_0^2$ at $\phi = 0$ or $2p\pi$ (p is integer). Irradiance has zero value for $N\phi/2 = p\pi$, where p is an integer with values neither zero nor a multiple of N . This makes ϕ

$= \frac{2p\pi}{N} = \pi ct/L$ or $t = (1/N)(2L/c)p$. Therefore, separation between two consecutive minima, that is, pulse width of a single laser pulse is $t = (1/N)(2L/c)$. Hence, the output of a mode-locked laser has sequence of short pulses of pulse duration $(1/N)(2L/c)$ separated in time by $2L/c$. The ratio of pulse separation to the pulse width is equal to the number of modes N , which shows that there should be a large number of modes in the cavity in order to get high-power short duration (picoseconds and femtoseconds) laser pulses.

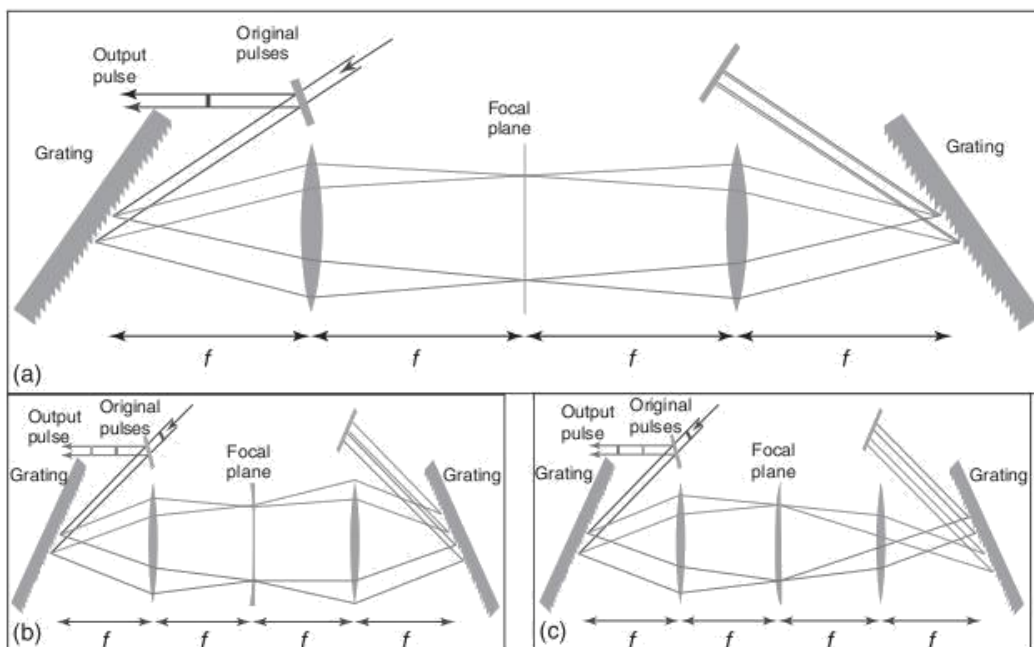


Figure: (a) Basic optical geometries for laser pulse shaping, (b) positive chirped and (c) negative chirped pulse shaping.

Laser Cutting Process

Laser cutting is used in manufacturing industries and is used for various materials. The materials absorb laser light and it comprises of cutting gas, cutting head, by-table as shown in figure 1.1 below. The laser light is transmitted from the optical fiber to the head (cutting head), the beam is then focussed on a single spot of the workpiece. The energy of the laser results in the melting of the material. The gas used pushes the material from the cut zone. The location of the workpiece is nearly 2mm from the cutting head.

Laser cutting is widely utilized in industry to produce complicated forms with tight tolerances. Laser cutting provides many benefits over traditional cutting, including a smaller heat impacted zone, more accuracy, the ability to process without physical touch, as well as a shorter processing time.

Laser cutting is being used by manufacturers to improve both the quality & the production of their products. Choice of suitable laser cutting factors like laser power, laser beam diameter, & cutting speed has a significant effect on productivity and quality. Matter & laser cutting parameters interact thermally and mechanically throughout the laser cutting process. HAZ is a term used to describe the area of the base material where heat created during laser cutting has altered the microstructure & mechanical characteristics, but the material itself has not yet melted. This shift in the area surrounding the cut surface is caused by heat created by the laser cutting process and then cooled. Fatigue resistance, surface cracking, & deformation may all occur in HAZ. To reduce heat impacted zones, it is important to pick the correct laser cutting settings[3].

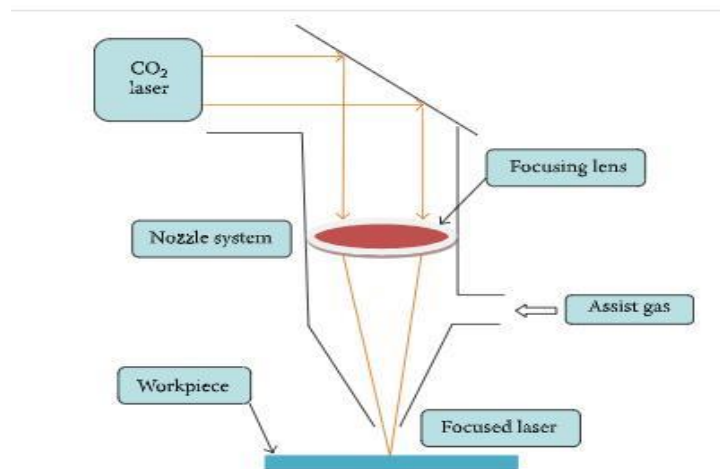


Figure 2: Experimental Setup for Laser Cutting Process

Advantages of Laser Cutting

Using lasers to cut materials has clear advantages:

- The ability to cut quickly
- High performance
- Wide variety of machining
- The cut is smooth while milling because a light beam substitutes the typical tool or flame. There is no need for further processing.
- The impacted region of reducing heat is modest.

- Deformation of a little sheet
- A thin cutting seam
- The incision is free of mechanical tension.
- There is no burr.
- High machining precision
- Repetitiveness is good
- Avoid scratching the plate's surface.
- CNC programming
- There is no need to remove the mold
- Time & money-saving

CAD Modelling

The specimen model is generated in Creo design software. This software is parametric and is specially meant for 3D cad modeling. The model is developed and converted into an integrated graphics file format (.iges). This file is imported into the ANSYS design modeler and checked for surface patches and other geometric errors as shown in figure 3 below. The dimensions of the specimen are 50mm * 25mm. The laser beam passes through colored slices in mid-portion.

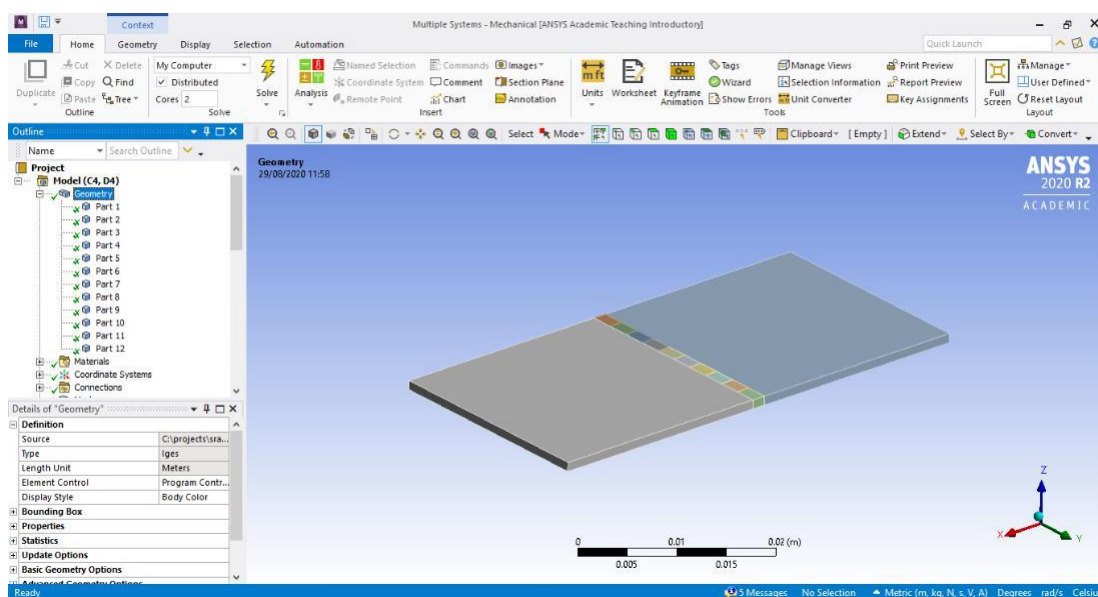


Figure 3: CAD model of the specimen

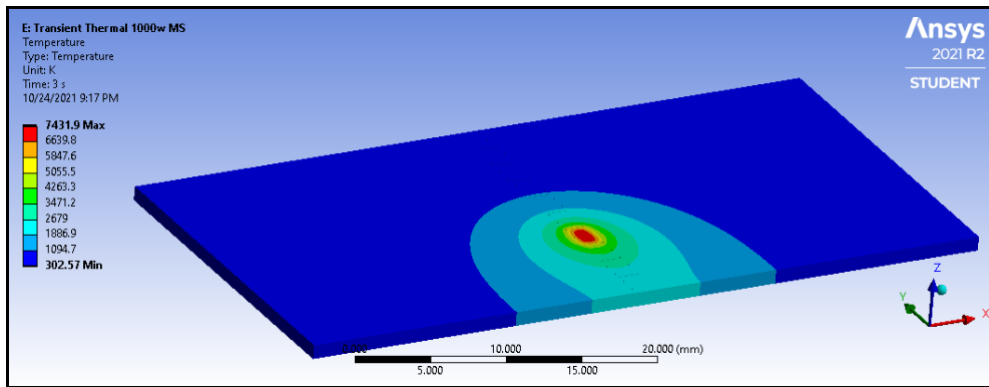


Figure 4: Temperature plot at 3 secs

Figure 4 above shows the temperature plot at 3 secs after laser cutting operation. The maximum temperature is 7431.9 °C and the minimum temperature is 1094.7°C. The temperature reduces as we move away from the cutting zone depicted by red color to light blue color.

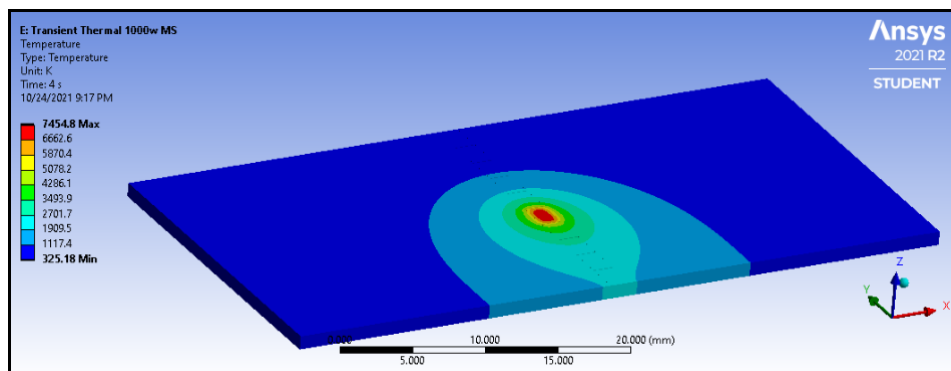


Figure 5: Temperature plot at 4 secs

Figure 5 above shows the temperature plot at 4 secs after laser cutting operation.

The maximum temperature is 7454.8°C and the minimum temperature is 1117.4°C.

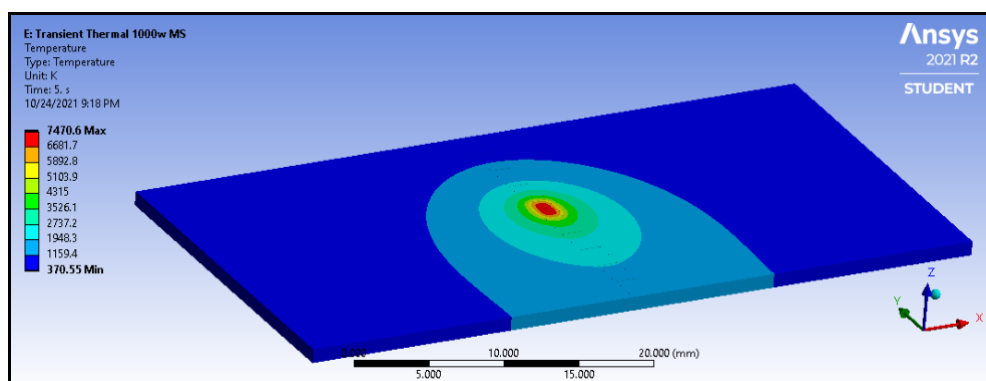


Figure 6: Temperature plot at 5 secs

Figure 6 above shows the temperature plot at 5 secs after laser cutting operation.

The maximum temperature is 7470.6°C and the minimum temperature is 1159.4°C.

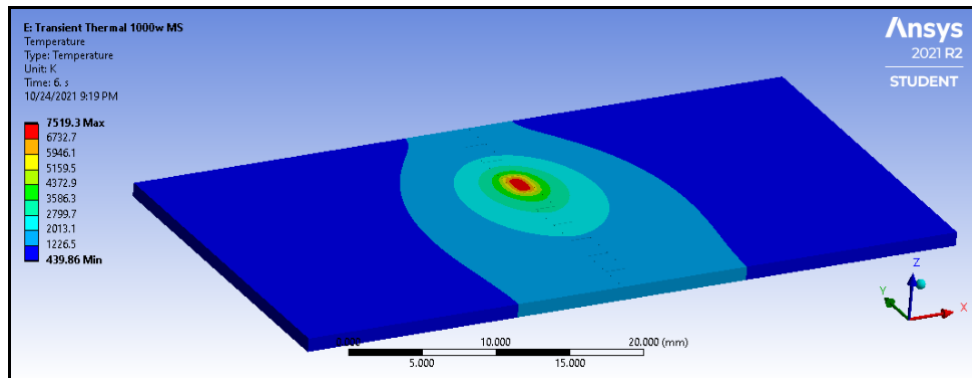


Figure 7: Temperature plot at 6 secs

Figure 7 above shows the temperature plot at 6 secs after laser cutting operation. The maximum temperature is 7519.3°C and the minimum temperature is 1226.5°C. The temperature reduces as we move away from the cutting zone depicted by red color to light blue color.

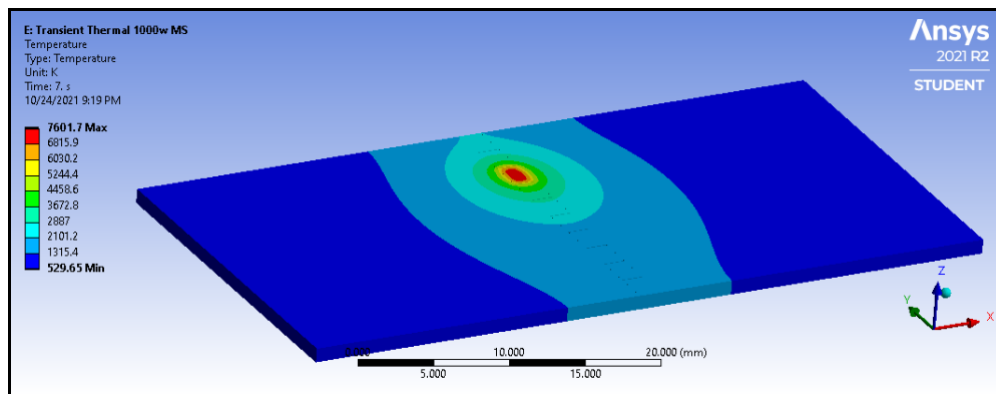


Figure 8: Temperature plot at 7 secs

Figure 8 above shows the temperature plot at 7 secs after laser cutting operation. The maximum temperature is 7601.7 °C and the minimum temperature is 1315.4°C. The temperature reduces as we move away from the cutting zone depicted by red color to light blue color.

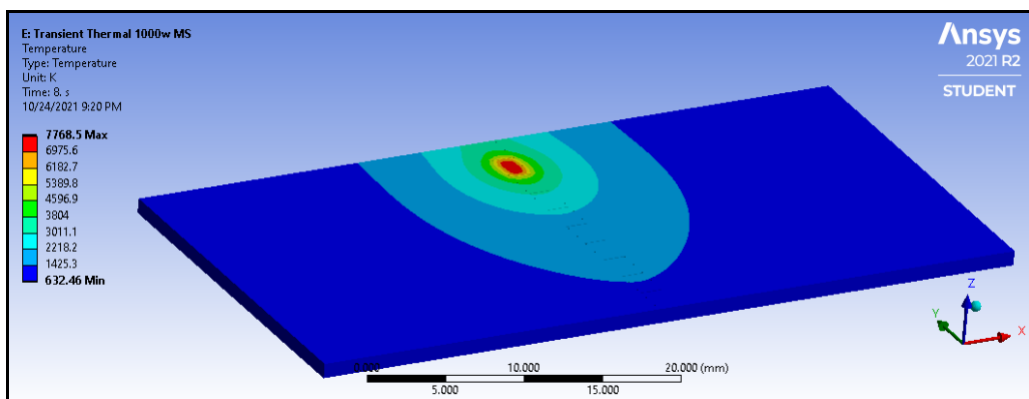


Figure 9: Temperature plot at 8 secs

Figure 9 above shows the temperature plot at 8 secs after laser cutting operation. The maximum temperature is 7768.5°C and the minimum temperature is 1423.5°C. The temperature reduces as we move away from the cutting zone depicted by red color to light blue color.

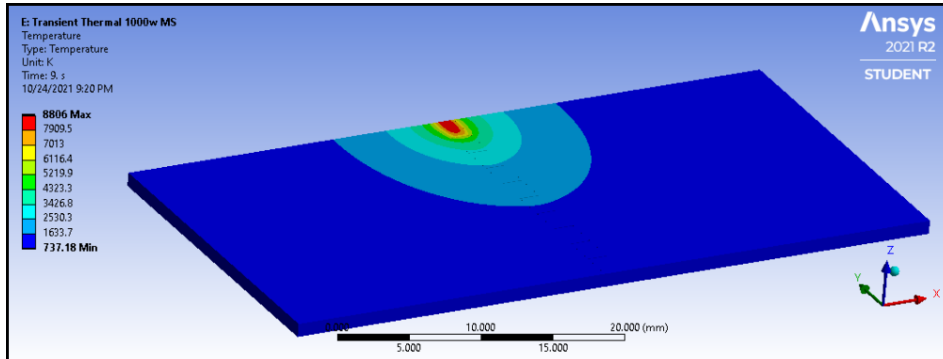


Figure 10: Temperature plot at 9 secs

Figure 10 above shows the temperature plot at 9 secs after laser cutting operation. The maximum temperature is 8806°C and the minimum temperature is 1633.7°C. The temperature reduces as we move away from the cutting zone depicted by red color to light blue color.

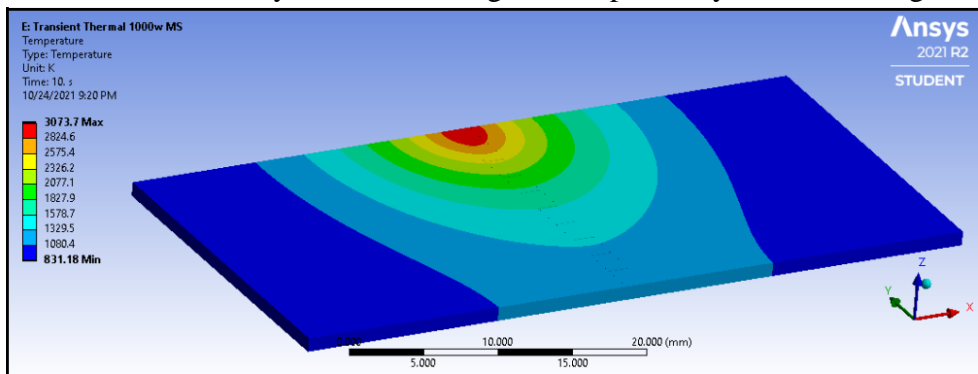


Figure 11: Temperature plot at 10 secs

Figure 11 above shows the temperature plot at 10 secs after laser cutting operation. The maximum temperature is 3073.7°C and the minimum temperature is 1080.4°C. The temperature reduces as we move away from the cutting zone depicted by red color to light blue color.

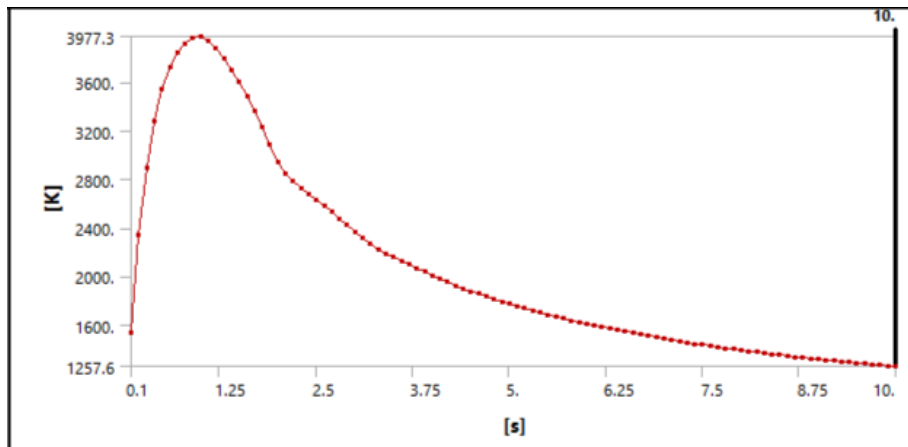


Figure 12: Temperature plot at 1mm distance

Figure 12 shows the temperature-time curve at a point 1mm away from the cutting zone which shows an increase in temperature up to 3977.3K and reduces to 1257.6K.

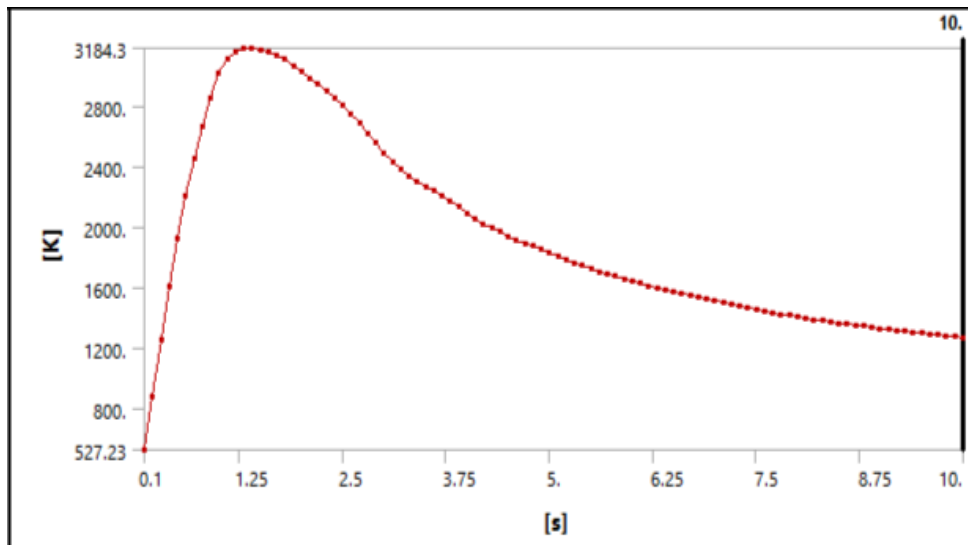


Figure 13: Temperature plot at 2mm distance

Figure 13 shows the temperature-time curve at a point 2mm away from the cutting zone which shows an increase in temperature up to 3184.3°C and reduces to 1400°C.

Conclusion

The FEA is a viable tool in determining the thermal characteristics of the composite material specimen on which laser beam is incident. The use of computer simulation can significantly reduce time and cost as against experimental techniques. The transient thermal analysis is conducted on a thin specimen made of composite materials i.e. CFRP, GFRP, PMMA, and structural steel. The temperature plot along with thermal stresses are determined. The detailed results areas:

1. The temperature distribution at the location of laser beam incidence is obtained.
2. The kerf width and HAZ are obtained for all the specimens i.e. CFRP, GFRP, PMMA, and structural steel.
3. The HAZ is highest for steel material and is minimum for PMMA and GFRP. The HAZ for PMMA and GFRP is limited to kerf width.
4. For CFRP material, the maximum temperature obtained at 1mm distance from laser beam incident is 5412.7K, and the maximum temperature at 2mm distance from laser beam incident is 3408.1K.

REFERENCES

- [1] T. Muangpool and S. Pullteap, "Reviews on laser cutting technology for industrial applications," no. November, p. 34, 2018, doi: 10.1117/12.2300955.
- [2] A. M. Sifullah, Y. Nukman, M. A. Hassan, and A. Hossain, "Finite element analysis of fusion laser cutting on stainless steel-304," *ARPN J. Eng. Appl. Sci.*, vol. 11, no. 1, pp. 181–189, 2016.
- [3] I. Miraoui, M. Boujelbene, and M. Zaied, "High-power laser cutting of steel plates: Heat affected zone analysis," *Adv. Mater. Sci. Eng.*, vol. 2016, 2016, doi: 10.1155/2016/1242565.
- [4] Shane, "5 Applications of Laser Technology in Industrial Production," *Machine MFG*, 2022. <https://www.machinemfg.com/laser-technology-applications/>.
- [5] E. K. CENTER., "How does the laser process work?," *ESAB KNOWLEDGE CENTER.*, 2021. <https://www.esabna.com/us/en/education/blog/laser-cutting-process.cfm/>.
- [6] F. Element and A. Using, "Finite Element Analysis Using ANSYS."
- [7] I. E. Reporting, "The Advantages of the Finite Element Method," *IEEE Innovation*, 2022. <https://innovationatwork.ieee.org/the-advantages-of-fem/>.
- [8] prashantsaini Shahanwazhavale, "What are the advantages and disadvantages of Finite element method.," *Ques10.* .
- [9] sanket shing ote Shaha nwaz havale, "Applications of Finite Element Method," *Ques10es10*, 2019. [https://www.ques10.com/p/23385/explain-the-application-of-fea-in-various-fields/#:~:text=Geotechnical engineering%3A FEM applications include,and dynamic soil structure interaction%5C](https://www.ques10.com/p/23385/explain-the-application-of-fea-in-various-fields/#:~:text=Geotechnical%20engineering%3A%20FEM%20applications%20include,and%20dynamic%20soil%20structure%20interaction%5C).

- [10] D. T. Academy, "Introduction to Ansys," *DesignTech system*, 2015. <https://www.designtechcadacademy.com/knowledge-base/ansys-software#:~:text=Ansys has been founded in,biomedical and other industrial sectors%5C>.
- [11] R. Potluri, "ANSYS Training: A Easy Introduction with Applications," *Udemy*, 2021. <https://www.udemy.com/course/fea-with-ansys-workbench/>.
- [12] I. OZEN ENGINEERING, "ANSYS ADVANTAGES," *OZEN ENGINEERING, INC.*, 2022. <https://www.ozeninc.com/about-ansys/ansys-advantages/#:~:text=Ansys provides you with the,within your company's user community%5C>.
- [13] ANSYS, "Applications of ANSYS," *ANSYS, Inc*, 2022. <https://www.ansys.com/en-in/applications%5C>.
- [14] D. Li, S. Hu, J. Shen, H. Zhang, and X. Bu, "Microstructure and Mechanical Properties of Laser-Welded Joints of Ti-22Al-25Nb / TA15 Dissimilar Titanium Alloys," *J. Mater. Eng. Perform.*, vol. 25, no. 5, pp. 1880–1888, 2016, doi: 10.1007/s11665-016-2025-4.
- [15] W. feng XU and Z. lin ZHANG, "Microstructure and mechanical properties of laser beam welded TC4/TA15 dissimilar joints," *Trans. Nonferrous Met. Soc. China (English Ed.)*, vol. 26, no. 12, pp. 3135–3146, 2016, doi: 10.1016/S1003-6326(16)64445-X.
- [16] Z. Gui, G. Min, D. Liu, and P. Hu, "Double-sided laser welding of dissimilar titanium alloys with linear variable thickness," 2015, doi: 10.1007/s00170-015-6922-8.

- [17] A. N. Cherepanov, A. M. Orishich, N. B. Pugacheva, and V. P. Shapeev,
“Investigation of the structure and properties of titanium – stainless steel permanent joints obtained by laser welding with the use of intermediate inserts and nanopowders *,” vol. 22, no. 2, pp. 135–142, 2015.
- [18] M. Degidi, D. Nardi, A. Morri, G. Sighinolfi, F. Tebbel, and C. Marchetti,
“Fatigue limits of titanium-bar joints made with the laser and the electric resistance welding techniques: microstructural characterization and hardness properties,” 2017, doi: 10.1177/0954411917709835.
- [19] H. Yu, F. Li, J. Yang, J. Shao, Z. Wang, and X. Zeng, “Investigation on laser welding of selective laser melted Ti-6Al-4V parts: Weldability, microstructure and mechanical properties,” *Mater. Sci. Eng. A*, vol. 712, no. November 2017, pp. 20–27, 2018, doi: 10.1016/j.msea.2017.11.086.